

# **Combustion and Energy Conversion Systems Laboratory**

**Laboratory Coordinator: Dr. Santanu De**

**Associated Faculty Members (if any):**

**List of Major Equipment:**

- Nd:YAG Laser with Chiller (Edgewave IS200)
- Tunable Dye Laser (Sirah Credo)
- CMOS Camera (Phantom VEO640)
- Gen II Image Intensifier (Lambart HiCatt2)
- Mass flow controllers (Alicat, Linetech, Qty: 8)
- Photomultiplier Tube (Thorlab)
- Gas-chromatograph (Nucon)
- Air compressor (Atlas Copco)
- Air dryer (Summit)
- Air dehumidifier (Bryair)
- 36 kW Inline Air Heater
- Electric heater (8 kW)
- Air pre-heater
- Steam boiler with superheater
- Coal pulverizer
- Muffle furnace
- Water Chiller
- Optical table (Newport)
- Peristaltic Pump
- Experimental rig of DFB gasifier
- Lab-Scale Liquid Fuel Combustor
- Lab-Scale Lean Premixed Gas Turbine Combustor

### Brief description of the laboratory:

Major research activities of the CECS laboratory can be classified under the following three verticals:

**Modeling of turbulent reactive flows:** Robust and computationally efficient models for turbulent combustion (flamelet, PDF, MMC methods) based on RANS/LES are being developed and applied to different non-premixed, premixed, and partially-premixed flames of gaseous and liquid fuels.

**Application of optical diagnostics tool to turbulent flames:** This involves using different line-of-sight and planar measurement techniques for flame visualization. The applications involve chemiluminescence and time-resolved planar laser-induced fluorescence imaging of flames and gas turbine combustors

**Coal and biomass gasification:** Fluidized bed gasification of high-ash coal and biomass (rice husk, straw, etc.) is being performed to produce syngas. The active research areas include optimizing operating parameters, hot cleaning of syngas, and membrane separation of H<sub>2</sub> and CO<sub>2</sub> capture.

### Laboratory research keywords:

Turbulent combustion; Spray combustion; Modeling of turbulent reactive flows; Gas turbine combustion; Laser-based optical diagnostics; Coal and biomass gasification; Fluidization; H<sub>2</sub> separation

### Major Research and Development Contribution of the Laboratory

Year	Major research and development activity
2020-2021	<ul style="list-style-type: none"><li>▪ <b>Time-resolved planar laser-induced fluorescence (PLIF) facility:</b> We have developed a state-of-the-art combustion diagnostics facility with a time-resolved planar laser-induced fluorescence (TR-PLIF) facility. The PLIF facility is being used to investigate many complex and transient turbulence-chemistry interaction phenomena in turbulent flames, gas turbine combustors, etc.</li><li>▪ <b>Development of lean premixed gas turbine combustor:</b> A lean-premixed, swirl-stabilized gas turbine combustor is developed with multiple injection ports. The combustor is commissioned and operated with a blend of CNG and H<sub>2</sub>. Chemiluminescence and TR-PLIF experiments are being performed.</li><li>▪ <b>Flow-blurring atomizer:</b> A flow-blurring atomizer is developed, and its spray is visualized based on the Mie-scattering technique. Significant improvement in atomization is found compared to conventional liquid fuel co-axial atomizer. Further characterization of the atomizer is being conducted for macroscopic and microscoping spray characterization.</li><li>▪ <b>A fully dynamic mixing timescale model for the sparse Lagrangian multiple mapping conditioning approach:</b> A novel variant of the minor mixing timescale model in MMC-LES, referred to herein as dyn-aISO, is proposed, and its performance is assessed by simulating the canonical</li></ul>

	<p>partially premixed, piloted flame series of Sandia exhibiting increasing levels of local extinction. The coefficients for modelling the sub-Lagrangian-filter scale scalar variance and scalar dissipation rates are dynamically modeled using local scalar field values. The new dynamic mixing timescale model could accurately predict the extinction and re-ignition phenomenon, requiring the micro-mixing model to produce the correct compositional fluctuations controlled by the minor mixing timescale model in the MMC method.</p> <ul style="list-style-type: none"> <li>▪ <b>Effects of drag and subgrid-scale turbulence modeling on gas-solid hydrodynamics of a pilot-scale circulating fluidized bed:</b> 3-D, full loop, LES of a circulating fluidized bed are conducted using EE approach. Effects of drag and sgs turbulence models are investigated. Results are validated against measurements from an in-house pilot-scale model. The influence of change in the riser diameter is more pronounced for EMMS models. The hybrid EMMS drag model and sgs-TKE model made the most accurate predictions.</li> <li>▪ <b>Energy, Exergy and Cost Analysis and Optimization of Hybridized Solar Power Tower Plant:</b> The performance of a hybridized solar power tower (SPT) plant in real-world scenarios is assessed, which has a north-facing HF that reflects and focuses light on a central cavity receiver. A combined cycle plant based on a close loop Helium Brayton cycle and two R123 organic Rankine cycles is simulated with a thermal energy storage system. An energy and exergy evaluation of the entire model is being conducted to examine the performance of various components.</li> </ul>
<p>2019-2020</p>	<ul style="list-style-type: none"> <li>▪ <b>Design and development of a pilot-scale bubbling fluidized bed gasifier for high ash coal:</b> Autothermal gasification of high-ash (&gt;45%) coal is conducted in a fluidized bed. The highest cold gas and carbon conversion efficiencies are 48% and 85%, respectively. A maximum value of syngas HHV of 3 MJ/Nm<sup>3</sup> is obtained during air-steam gasification. An optimum range of steam/coal ratio is found in the range of 0.19–0.28, which maintains bed temperature in the range of 800-900°C. Despite having low alkali content in ash, agglomerates form due to local hotspots. At low fluidization numbers, agglomerates are formed due to local hotspots, as the collected ash sample has small alkali content.</li> <li>▪ <b>Investigation of cold flow hydrodynamics in a dual fluidized bed for gasification of high-ash coal:</b> A compact DFB model with short riser is proposed for gasification of high-ash coal. The bottom bed of riser is operated in BFB and FFB regimes using primary aeration. Effect of on-bed and in-bed solids discharge from BFB to the riser is investigated. The role of secondary aeration on solids circulation and solids holdup is studied.</li> <li>▪ <b>Investigation of hydrodynamics and segregation characteristics in a dual fluidized bed using the binary mixture of sand and high-ash coal:</b> A compact dual fluidized bed with a short riser has been investigated. Effects of unary sand and polydisperse coal/sand binary mixture are investigated. Gas leakage is examined for single chamber pot-seal and double chamber loop-seal. A hydrodynamic model is established to predict axial solids holdup in the riser.</li> </ul>

	<ul style="list-style-type: none"> <li>▪ <b>Numerical investigation of cold flow hydrodynamics in an internally circulating dual fluidized bed for coal gasification:</b> Cold flow hydrodynamic study of a full loop, three-dimensional internally circulating dual fluidized bed (ICDFB) for coal gasification has been carried out using a Eulerian–Eulerian approach. The ICDFB system consists of a central riser and an annular bubbling fluidized bed (BFB) placed concentrically and interconnected by a solids separator and a loop seal. A sensitivity study of various operating parameters that potentially influence solids distribution and recirculation rate has been conducted. The riser gas superficial velocity and loop-seal aeration rate are found to be the major controlling factors of solids recirculation rate.</li> <li>▪ <b>Large eddy simulation of biomass gasification in a bubbling fluidized bed based on the multiphase particle-in-cell method:</b> A hybrid EL solver is developed for gas-solids flows based on MP-PIC framework. Gasification of rice husk in a bubbling fluidized bed is performed. The solver could capture transient flow characteristics of gas-solids flows. Product gas compositions show a good agreement with the experimental measurements. Effects of temperature, steam-to-biomass ratio, and equivalence ratio are studied.</li> <li>▪ <b>LES of a lifted methanol spray flame series using the sparse Lagrangian MMC approach:</b> Two-phase multiple mapping conditioning / large eddy simulation (MMC-LES) is applied for the first time to lifted spray flames on a vitiated coflow burner. Three flames with different inlet fuel mass loading are investigated. MMC-LES uses a hybrid Eulerian-Lagrangian-Lagrangian approach for the evolution of gas-phase flow, stochastic particles, and liquid fuel droplets, respectively. Two distinct flame base stabilization phenomena are observed, namely a flat flame base spreading across the central region of the jet at low and intermediate fuel loading cases, and an annular flame base in the shear layer that surrounds a cold central jet region, a characteristic of autoignition due to entrainment of hot oxidizer from the co-flow for the highest fuel loading case.</li> </ul>
<p><b>2018-2019</b></p>	<ul style="list-style-type: none"> <li>▪ <b>Numerical investigation of flow and scalar fields of piloted, partially-premixed dimethyl ether/air jet flames:</b> The computed conditional and unconditional statistics based on the RANS-stochastic MMC approach demonstrate an excellent agreement with the available experimental data, even for flame displaying a large degree of local extinction and re-ignition. For these flames, radical species distribution conditioned on mixture fraction confirms the physical separation between the OH and CH<sub>2</sub>O species, which was earlier reported using simultaneous laser-induced fluorescence measurements of these radicals. A distinct separation between these radicals becomes evident at downstream locations where the scalar dissipation rate decreases. For the flames investigated here, a strong correlation is noticed between the peak heat release rate and the reaction rate indicator, <math>R_{OH}</math> based on the product of concentrations of OH and CH<sub>2</sub>O radicals.</li> <li>▪ <b>Numerical simulation of lifted DME jet diffusion flames using sparse Lagrangian MMC approach:</b> A series of simulations are performed for different coflow temperatures (1275 – 1500 K) for pure DME jets issued in</li> </ul>

	<p>a vitiated co-flowing oxidizer stream consisting of products from a lean, premixed H<sub>2</sub>-air combustion. The variation in the lift-off height (LOH) has been captured adequately and the reported trend agrees with the experimental data. Further, the flame structure has been analyzed in terms of the conditional scatter data of OH and CH<sub>2</sub>O radicals. In these flames, OH is formed in the shear layer of the jet and the coflow, whereas CH<sub>2</sub>O is found in the fuel-rich region of the jet. Near the flame base, OH and CH<sub>2</sub>O are found to significantly overlap with each other, whereas a distinct separation is noticed downstream of the flame base.</p> <ul style="list-style-type: none"> <li>▪ LES-FPV approach for kerosene-fueled scramjet engine</li> <li>▪ Numerical Investigation of Steady and Unsteady Combustion Phenomena in a 100 kW Micro Gas Turbine</li> <li>▪ Large eddy simulation of biomass gasification in a bubbling fluidized bed based on the multiphase particle-in-cell method</li> </ul>
<p><b>2017-2018</b></p>	<ul style="list-style-type: none"> <li>▪ <b>RANS-based stochastic MMC approach of auto-igniting turbulent lifted CH<sub>4</sub>/air jet diffusion flames in a vitiated co-flow:</b> In MMC, the concept of the mapping function is used, which approximates the cumulative probability distribution of the major scalar, namely mixture fraction for nonpremixed combustion. The corresponding variance of the major scalar is modelled by choosing a standard implementation of the major mixing time scale <math>\tau_\phi</math> modelled in terms of the turbulent time scale as <math>\tau_\phi = \tau_t/C_\phi</math>. The same major mixing time constant <math>C_\phi = 3.0</math> is used for all simulations. Additionally, in MMC, a minor mixing timescale <math>\tau_{\min}</math> is introduced, which controls fluctuations of scalars relative to the major fluctuations via the minor mixing time constant, <math>C_{\min}</math>. Three different values of <math>C_{\min} = \tau_{\min}/\tau_\phi = 0.25, 0.35</math> and <math>0.5</math> are used and the corresponding ratios of minor to turbulent time scales are <math>\tau_{\min}/\tau_t = 0.083, 0.116</math> and <math>0.166</math>, respectively. The conditional and unconditional reactive scalar fields are highly dependent on the choice of <math>C_{\min}</math> and hence the ratio of the minor and major mixing time scales. The variation in lift-off height is in good agreement with the experimental data for the entire range of coflow temperature for <math>C_{\min} = 0.25</math>.</li> <li>▪ Hydrodynamics Study of Fluidized Bed Gasifiers Using an Eulerian-Eulerian Approach</li> <li>▪ Aerodynamic design optimization of a centrifugal compressor impeller for micro gas turbine</li> <li>▪ Numerical Simulations of Turbulent Lifted Jet Diffusion Flames using Stochastic Multiple Mapping Conditioning Approach</li> <li>▪ LES based <math>\Sigma - Y</math> model for primary atomization using Eulerian stochastic fields approach</li> </ul>
<p><b>2016-2017</b></p>	<ul style="list-style-type: none"> <li>▪ <b>Numerical simulations of turbulent lifted jet diffusion flames in a vitiated coflow using RANS-based stochastic MMC approach:</b> Lifted turbulent jet diffusion flames of H<sub>2</sub>/N<sub>2</sub> issued into a hot coflowing stream of combustion products from a lean premixed H<sub>2</sub>/air mixture are</li> </ul>

	<p>simulated using RANS-MMC approach. The MMC approach emulates large-scale turbulent fluctuations by using a reference variable, mixture fraction. The modified Curl's model has been adapted to model the micro-mixing term. The computed results from the present simulations are in excellent agreement with the available experimental data. The flame lift-off heights obtained using the minor mixing time constant <math>C_{\min} = 0.25</math> are found to be in close proximity with the experimentally observed values for the entire range of coflow temperatures.</p> <ul style="list-style-type: none"> <li>▪ <b>Numerical modeling of turbulent premixed combustion using RANS-MMC approach:</b> The Sydney piloted premixed jet burner (PPJB) operating in the distributed combustion regime has been considered for model validation. The reaction progress variable is chosen as the reference variable in RANS-MMC of premixed combustion. The stochastic MMC solver has been fully integrated with the RANS flow solver. Computed radial profiles of the mean axial velocity and species mass fractions agree with the available experimental data. In some instances, the RANS-MMC model matches the experimental data better than the results obtained from other state-of-the-art turbulent combustion models.</li> </ul>
<p><b>2015-2016</b></p>	<ul style="list-style-type: none"> <li>▪ <b>Flame stabilization of turbulent lifted H<sub>2</sub> flames in vitiated coflow using RANS-CMC approach:</b> H<sub>2</sub> flames in vitiated coflow is simulated. RANS-CMC approach is used to study flame stabilization. Effect of jet velocity, coflow velocity, coflow temperature and mixing is studied.</li> <li>▪ <b>Development of an OpenFOAM-based solver for SCRAMJET combustion:</b> Large eddy simulations for a hydrogen-fuelled DLR scramjet combustor have been performed using the dynamic Smagorinsky model with the Lagrangian averaging technique. Both non-reacting and reacting cases have been investigated. The physical configuration corresponds to the scramjet combustor experimentally investigated at the Institute for Chemical Propulsion of the German Aerospace Center (DLR). Favre-averaged transport equations for mass, momentum, energy and species concentrations are solved using a finite volume discretization scheme in OpenFoam. The single-step global reaction is used for the partially stirred reactor (PaSR) combustion model. Numerical results for time-averaged pressure, temperature, and axial velocity are compared with experimental data at different cross-sections of the combustor.</li> </ul>

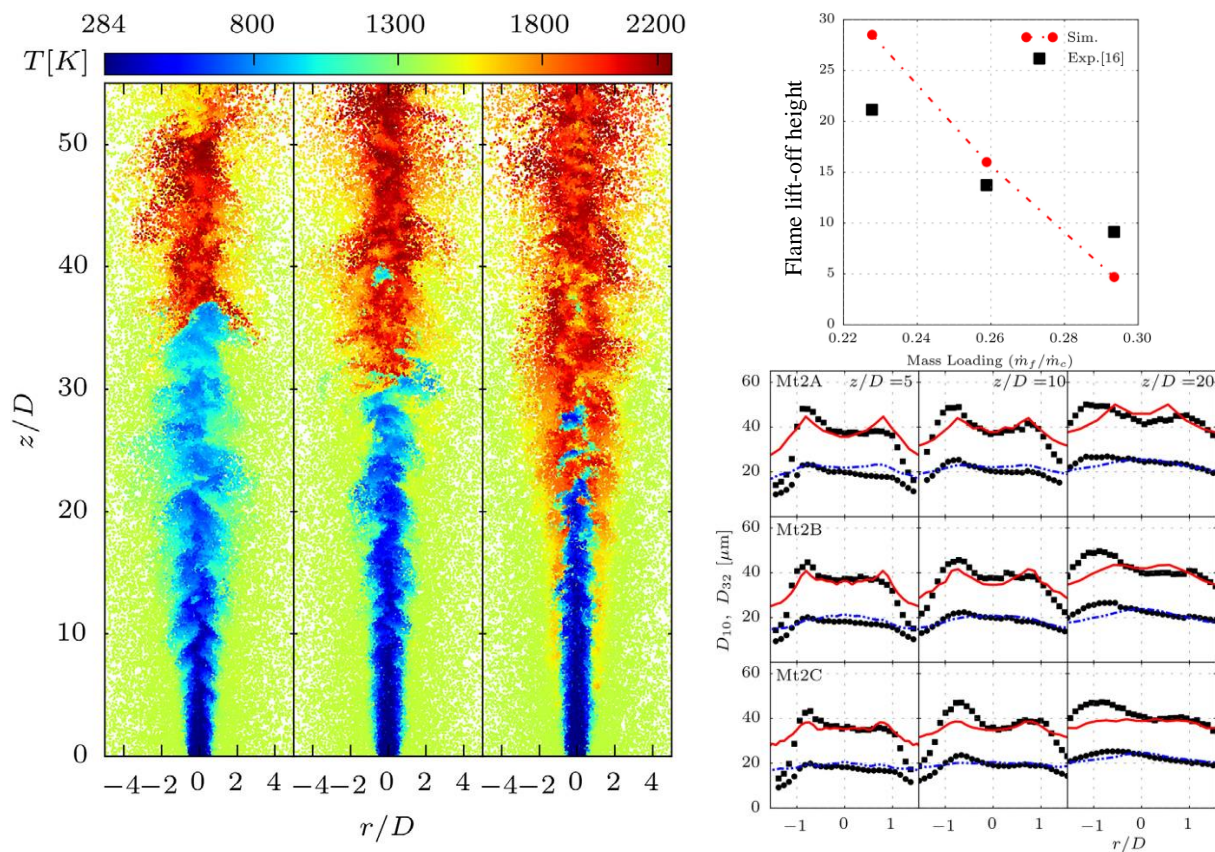


Figure #1: MMC-LES of methanol spray flames: Instantaneous temperature of stochastic particles clipped at the mid-plane (left), flame lift-off height vs. fuel mass loading (right-top), spray AMD and SMD distribution (right-bottom) (Sharma et al., 2021, Proci. Combust. Inst. 38 (2), 3399-3407)

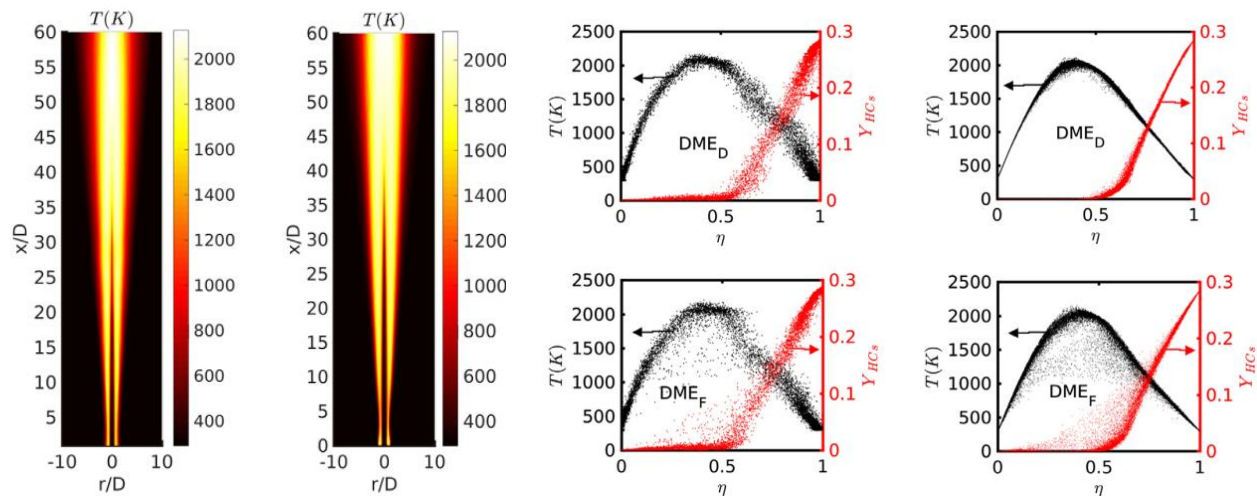
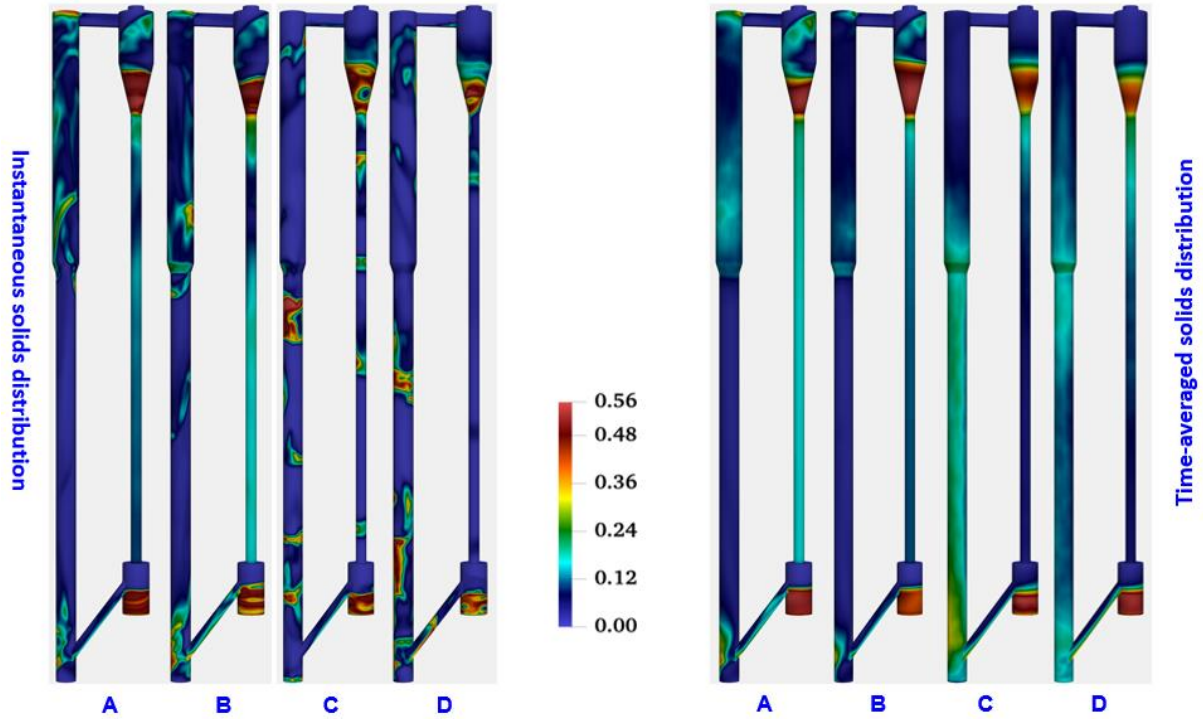


Figure #2: RANS-MMC simulation of DME D and F flames: average temperature (left), conditional temperature (right) (Ghai and De, 2019, Combust. Flame 208, 480-491).



A: Gidaspow; B: Syamlal O'Brien; C: EMMS; D: hybrid-EMMS

Figure #3: Effect of drag models on numerical simulation of circulating fluidized bed: instantaneous (left) and time-averaged (right) solid distribution (Gupta et al., 2022, Chem. Engg. Sci. 248, 117093)

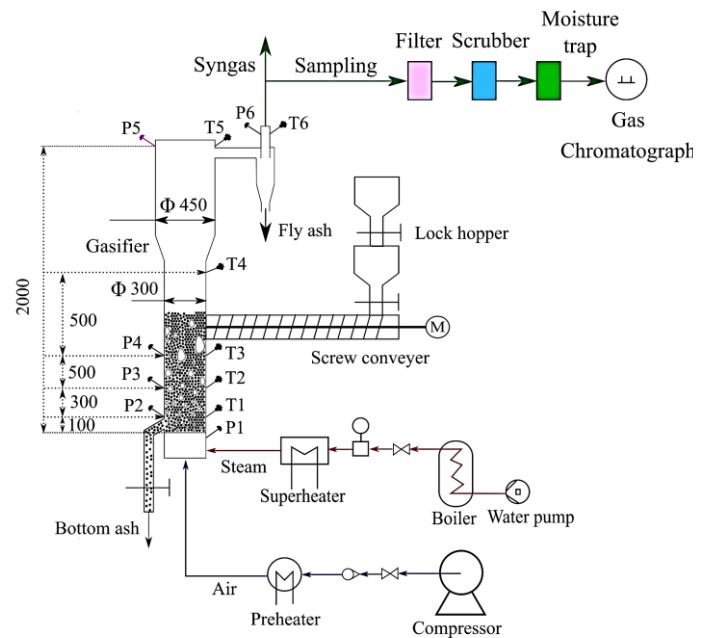


Figure #4: 300 kW<sub>th</sub> fluidized bed gasifier of high-ash coal: actual photograph (left), schematic diagram (right) (Gupta and De, 2022, Energy 244, 122868)



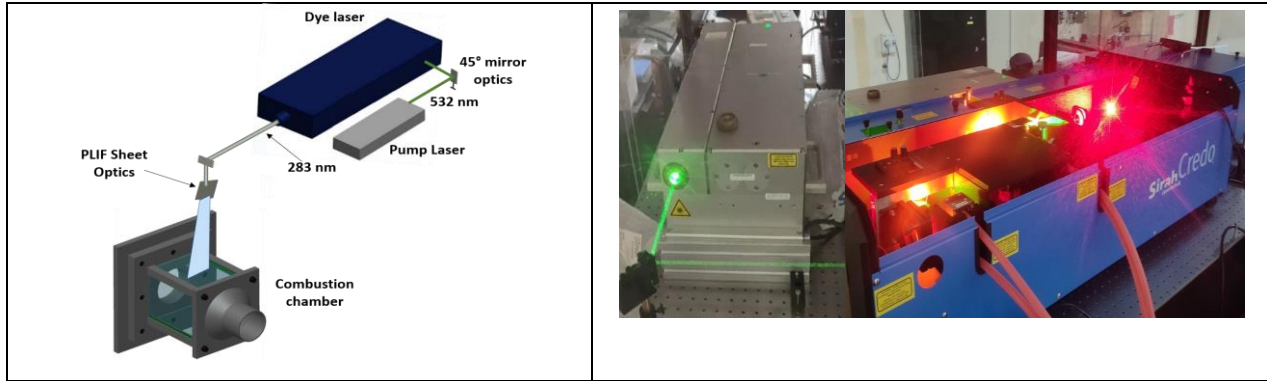


Figure #5: A schematic diagram of time-resolved planar laser-induced fluorescence (PLIF) setup (left), actual images of the pump laser and dye laser (right)

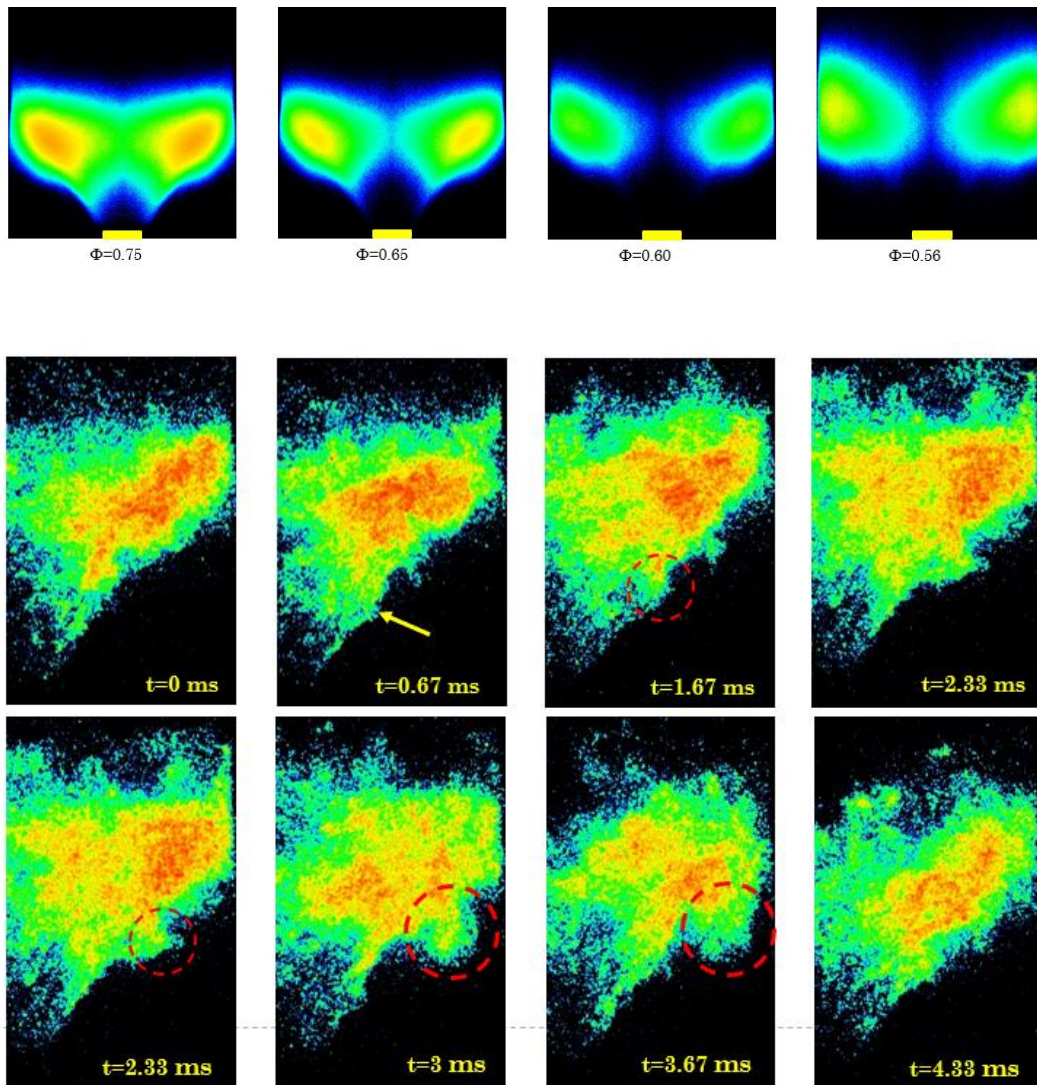


Figure #6: OH chemiluminescence images of a lean premixed combustor: average images at different equivalence ratio ( $\phi$ ) (top row), sequence of instantaneous OH images for  $\phi = 0.75$  showing unsteady events (bottom row)